Constrained damped mass-spring system

T. Stykel

Technische Universität Berlin

Consider the holonomically constrained damped mass-spring system [1] shown in Fig. 1.

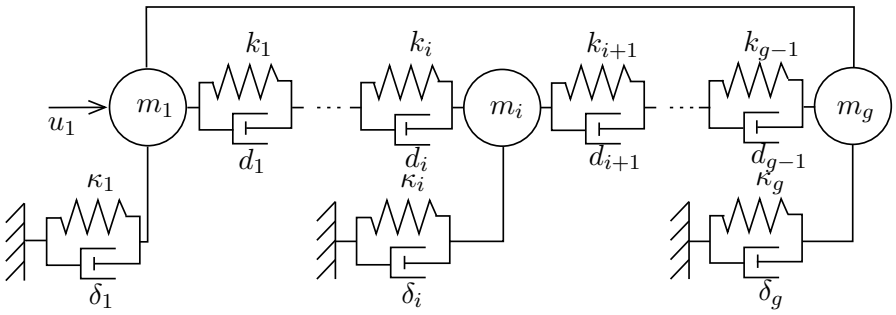

Figure 1: A damped mass-spring system with a holonomic constraint.

The ith mass of weight m_i is connected to the $(i+1)$st mass by a spring and a damper with constants k_i and d_i, respectively, and also to the ground by a spring and a damper with constants κ_i and δ_i, respectively. Additionally, the first mass is connected to the last one by a rigid bar and it is controlled. The vibration of this system is described by a descriptor system

$$\begin{aligned} \dot{\mathbf{p}}(t) &= \mathbf{v}(t), \\ M\dot{\mathbf{v}}(t) &= K\,\mathbf{p}(t) + D\mathbf{v}(t) - G^T\boldsymbol{\lambda}(t) + B_2u(t), \\ 0 &= G\,\mathbf{p}(t), \\ y(t) &= C_1\mathbf{p}(t), \end{aligned} \tag{1}$$

where $\mathbf{p}(t) \in \mathbb{R}^g$ is the position vector, $\mathbf{v}(t) \in \mathbb{R}^g$ is the velocity vector, $\boldsymbol{\lambda}(t) \in \mathbb{R}^2$ is the Lagrange multiplier, $M = \operatorname{diag}(m_1, \ldots, m_g)$ is the mass matrix,

$$D = \begin{bmatrix} \delta_1 + d_1 & -d_1 & & & & 0 \\ -d_1 & d_1 + \delta_2 + d_2 & \ddots & & & \\ & \ddots & \ddots & \ddots & & \\ & & -d_{s-2} & d_{s-1} + \delta_{s-1} + d_{k-1} & -d_{s-1} & \\ 0 & & & -d_{s-1} & d_{s-1} + \delta_s & \end{bmatrix}$$

the damping matrix,

$$K = \begin{bmatrix} \kappa_1 + k_1 & -k_1 & & & & 0 \\ -k_1 & k_1 + \kappa_2 + k_2 & \ddots & & & \\ & \ddots & \ddots & \ddots & & \\ & & -k_{s-2} & k_{s-1} + \kappa_{s-1} + k_{k-1} & -k_{s-1} & \\ 0 & & & -k_{s-1} & k_{s-1} + \kappa_s & \end{bmatrix}$$

the stiffness matrix, $G = [\,1, 0, \ldots, 0, -1\,] \in \mathbb{R}^{1,g}$ is the constraint matrix, $B_2 = e_1$ and $C_1 = [\,e_1,\ e_2,\ e_{g-1}\,]^T$. Here e_i denotes the ith column of the identity matrix I_g.

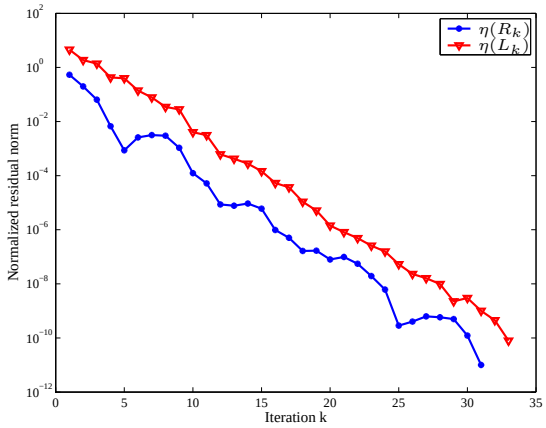

Figure 2: Convergence history for the normalized residuals $\eta(R_k) = \eta(E, A, P_l B; R_k)$ and $\eta(L_k) = \eta(E^T, A^T, P_r^T C^T; L_k)$.

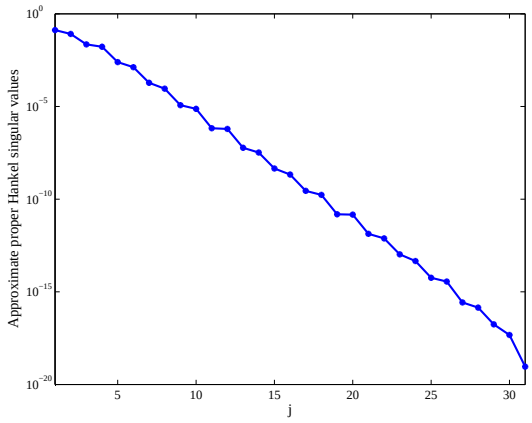

Figure 3: Approximate proper Hankel singular values for the damped mass-spring system.

The descriptor system (1) is of index 3 and the projections P_l and P_r can be computed as

$$P_l = \begin{bmatrix} \Pi_1 & 0 & -\Pi_1 M^{-1} D G_1 \\ -\Pi_1^T D(I - \Pi_1) & \Pi_1^T & -\Pi_1^T (K + D\Pi_1 M^{-1} D) G_1 \\ 0 & 0 & 0 \end{bmatrix},$$

$$P_r = \begin{bmatrix} \Pi_1 & 0 & 0 \\ -\Pi_1 M^{-1} D(I - \Pi_1) & \Pi_1 & 0 \\ G_1^T (K\Pi_1 - D\Pi_1 M^{-1} D(I - \Pi_1)) & G_1^T D\Pi_1 & 0 \end{bmatrix},$$

where $G_1 = M^{-1} G^T (G M^{-1} G^T)^{-1}$ and $\Pi_1 = I - G_1 G$ is a projection onto $\mathrm{Ker}\,(G)$ along $\mathrm{Im}\,(M^{-1} G^T)$, see [2].

In our experiments we take $m_1 = \ldots = m_g = 100$ and

$$\begin{aligned} k_1 = \ldots = k_{g-1} = \kappa_2 = \ldots = \kappa_{g-1} = 2, \quad \kappa_1 = \kappa_g = 4, \\ d_1 = \ldots = d_{g-1} = \delta_2 = \ldots = \delta_{g-1} = 5, \quad \delta_1 = \delta_g = 10. \end{aligned}$$

For $g = 6000$, we obtain the descriptor system of order $n = 12001$ with $m = 1$ input and $p = 3$ outputs. The dimensions of the deflating subspaces of the pencil corresponding to the finite and infinite eigenvalues are $n_f = 11998$ and $n_\infty = 3$, respectively.

Figure 2 shows the normalized residual norms for the low rank Cholesky factors R_k and L_k of the proper Gramians computed by the generalized ADI method with 20 shift parameters. The approximate dominant proper Hankel singular values presented in Fig. 3 have been determined from the singular value decomposition of the matrix $L_{33}^T E R_{31}$ with $L_{33} \in \mathbb{R}^{n,99}$ and $R_{31} \in \mathbb{R}^{n,31}$. All improper Hankel singular values are zero. This implies that the transfer function $\mathbf{G}(s)$ of (1) is proper. We approximate the descriptor system (1) by a standard state space system of order $\ell = \ell_f = 10$ computed by the approximate GSR method. In Fig. 4 we display the magnitude and phase plots of the $(3, 1)$ components of the frequency responses $\mathbf{G}(i\omega)$ and $\widetilde{\mathbf{G}}(i\omega)$. Note that there is no visible difference between the magnitude plots for the full order and reduced-order systems. Similar results have been observed for other components of the frequency response. Figure 6 show the absolute error $\|\mathbf{G}(i\omega) - \widetilde{\mathbf{G}}(i\omega)\|_2$ for a frequency

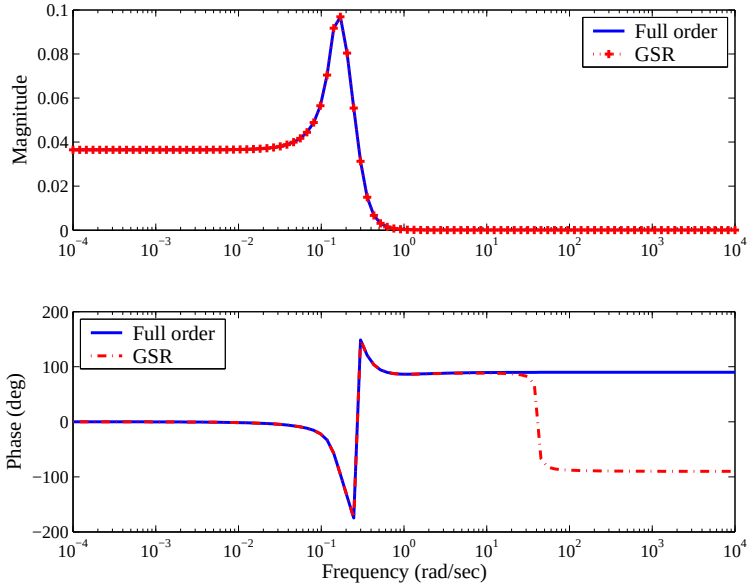

Figure 4: Magnitude and phase plots of $G_{31}(i\omega)$ for the damped mass-spring system.

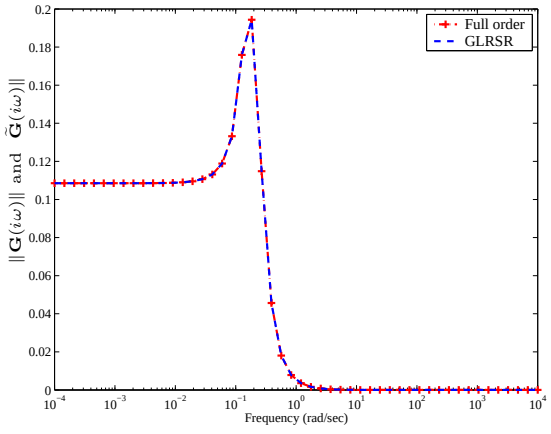

Figure 5: The spectral norms of the frequency responses $\mathbf{G}(i\omega)$ and $\widetilde{\mathbf{G}}(i\omega)$.

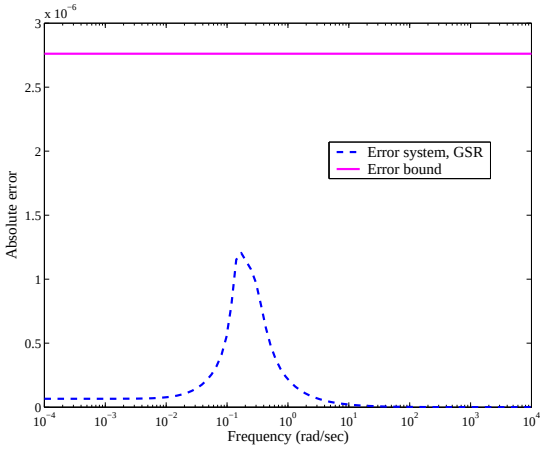

Figure 6: Absolute error plot and error bound for the damped mass-spring system.

rang $\omega \in [\,10^{-4},\ 10^{4}\,]$ and the approximate error bound computed as twice the sum of the truncated approximate proper Hankel singular values. We see that the reduced-order system approximates the original system satisfactorily.

References

[1] V. Mehrmann and T. Stykel. Balanced truncation model reduction for large-scale systems in descriptor form. In P. Benner, V. Mehrmann, and D. Sorensen, editors, *Dimension Reduction of Large-Scale Systems*, volume 45 of *Lecture Notes in Computational Science and Engineering*, pages 83–115. Springer-Verlag, Berlin/Heidelberg, 2005.

[2] R. Schüpphaus. *Regelungstechnische Analyse und Synthese von Mehrkörpersystemen in Deskriptorform*. Ph.D. thesis, Fachbereich Sicherheitstechnik, Bergische Universität-Gesamthochschule Wuppertal. Fortschritt-Berichte VDI, Reihe 8, Nr. 478. VDI Verlag, Düsseldorf, 1995. [German].